

Intersublevel polaron laser with InAs/GaAs self-assembled quantum dots

S. Sauvage^{a)} and P. Boucaud

Institut d'Électronique Fondamentale CNRS UMR8622, Université Paris-XI, 91405 Orsay, France

(Received 10 October 2005; accepted 15 December 2005; published online 7 February 2006)

We propose a three-level scheme to achieve intersublevel population inversion, optical gain, and intersublevel lasing effect in *n*-doped InAs/GaAs self-assembled quantum dots under optical pumping. The proposed Ruby-type laser scheme uses the natural splitting of the *s-p* polaron intersublevel transitions around 25 μm wavelength. The relaxation time engineering, which leads to optical gain in the system, relies (i) on the slow polaron relaxation from the P_- state down to the S ground state, governed by the specific strong coupling regime for the electron-phonon Fröhlich interaction and (ii) on the fast nonradiative relaxation of the polaron between the P_+ and P_- levels through the irreversible emission of acoustic phonons. TE-polarized optical gain up to 330 cm^{-1} is calculated for 80 quantum dot planes in an in-plane monomode waveguide geometry and a laser pump intensity threshold as low as 930 W/cm^2 , two orders of magnitude smaller than for quantum wells, is predicted. © 2006 American Institute of Physics. [DOI: 10.1063/1.2169919]

Quantum cascade lasers (QCLs) are quantum well (QW) based unipolar lasers that have been tremendously suited in providing versatile emission in the mid- and far-infrared spectral range to cover a wide diversity of potential applications.^{1,2} Intersubband transitions (ISBTs) in QWs have been extensively used to demonstrate laser emission in a variety of materials, in pulsed and continuous modes, at temperatures below and above 300 K and for wavelength ranges extending presently towards the terahertz range.³ Quantum cascade lasers have mainly profited from the one-dimensional confinement of the carriers in QWs and the wave function and relaxation time engineering that follows.

Quantum dots (QDs) also exhibit intraband transitions, also called intersublevel transitions (ISLTs), in the mid- and far-infrared. Contrarily to ISBTs in QWs, ISLTs in QDs are dynamically (and also spectrally) ruled by the specific strong electron-phonon coupling,^{4,5} that leads to the formation of mixed electron-phonon entangled quasiparticles as the eigenstates of the system, i.e., polarons. Several improvements for an ISLT based laser in QDs can be *a priori* expected as compared to ISBTs in QWs. ISLTs are not limited to vertical polarization and exhibit strong *in-plane* polarized dipoles forbidden in the conduction band of QWs. Relaxation is slowed down as a consequence of the state density reduction and the polaron formation. Relatively long $T1$ relaxation times, in the tens of picoseconds (ps) regime, have been reported, one to two orders of magnitude longer than in QWs.⁶ Large relaxation time difference between confined levels has been measured.⁷ Recently measurements also reported relatively long $T2$ dephasing times of the order of 5 ps, one order of magnitude longer than in quantum wells, expected to lead to lower optical intensity or current density thresholds.⁸ At last the three-dimensional confinement of the carriers avoids strong free carrier absorption in the midinfrared. So far QD intersublevel lasers have only been proposed and discussed theoretically, but without an appropriate treatment of quantum dot dynamics related to the strong electron-phonon coupling regime.^{9–11} In this letter, we propose a three-level scheme to achieve optical gain under optical pumping in

currently *experimentally investigated* InAs/GaAs self-assembled quantum dots. We predict laser effect using realistic experimental input figures that can be found in the literature for InAs/GaAs self-assembled QDs.

Figure 1 depicts the proposed level system that provides population inversion and optical gain. It is based on the typical polaronic structure of a flat-shape InAs/GaAs self-assembled quantum dot as calculated in Refs. 12 and 19. The polaron states are calculated from the electronic structure (energies, envelope wave functions) deduced from the three-dimensional resolution of the Schrödinger equation written in 8 band $\mathbf{k}\cdot\mathbf{p}$ theory¹² for a flat inverted pyramidal $15.5 \times 16.3 \times 2.5$ nm quantum dot and from the strong electron-phonon coupling following Refs. 13 and 14 considering only a monochromatic one LO-phonon continuum. Spin splitting is disregarded. Piezoelectricity is not considered. The strong coupling leads to entangled electron-phonon states as the eigenstates of the system. The mainly electronic excited states P_+ and P_- , predicted at 50 and 55 meV, are split because of the 5% [010] elongation chosen for the quantum dots. Note that such a splitting is actually observed experimentally using midinfrared absorption spectroscopy, as a result of shape anisotropy, piezoelectricity, and crystal symmetry.^{5,7,15,20} The formation of polarons also creates ad-

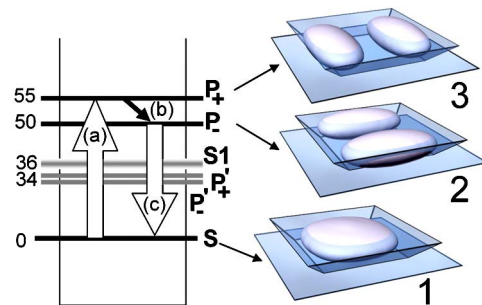


FIG. 1. Ruby-type three-level scheme for a QD intersublevel polaron laser. The three arrows indicate the optically pumped transition (a), the fast non-radiative relaxation transition (b), and the intersublevel lasing transition (c). The relative energy of each discrete or continuum levels are indicated on the left. The envelope wave functions of the main electronic component S , P_+ , and P_- are represented on the right. Piezoelectricity is not considered.

^{a)}Electronic mail: sebastien.sauvage@ief.u-psud.fr

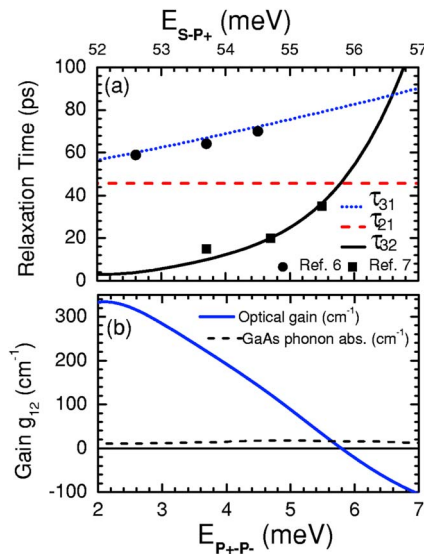


FIG. 2. Calculated relaxation times τ_{21} , τ_{31} , and τ_{32} (a) and optical gain (b) as a function of P_+ - P_- separation energy for a fixed S - P_- transition energy $E_{27}^0 = 50$ meV. Three experimental estimations of τ_{31} in Ref. 6 and τ_{32} in Ref. 7 are reported as symbols. The experimental GaAs two phonon absorption measured in Ref. 24 is also reported as a thin black line.

ditional states in the polaronic structure as compared to the electronic structure; P'_+ and P'_- states are mainly phononic, orthogonal to the P_+ and P_- states and are very close to the LO phonon uncoupled continuum at 36 meV.

The three arrows in Fig. 1 represent the three key ISLTs involved in the laser scheme: the optically pumped transition (a), the fast nonradiative relaxation transition (b), and the laser transition (c). Population inversion is expected to occur between the excited P_- polaron state and the S ground state. This scheme is significantly different from what is usually considered in QCLs where $3 \rightarrow 2$ would be the lasing transition and $2 \rightarrow 1$ a fast relaxing transition draining the carriers out of the period. The scheme actually mimics the original Ruby laser where level 2 corresponds to the metastable state.¹⁶ A key feature of the scheme is the forbidden relaxation from P_+ or P_- to the intermediate states P'_- and P'_+ due to the vanishing anharmonic matrix element permitting relaxation only towards the ground state. The optical pumping of transition (a) could be achieved in practice with a suitable quantum cascade laser around 23 μm wavelength¹⁷ or a picosecond free electron laser for stimulated emission investigation as it has already been done for quantum wells.¹⁸ The electronic structure could also be tuned in resonance to presently available pump laser wavelengths, e.g., using vertically electronically coupled QDs.¹⁹ However, in this letter we will disregard the practical and important issue of optical pumping and we will rather focus on the predicted properties of such an optically pumped system.

Figure 2(a) shows the three main relaxation times τ_{21} , τ_{32} , and τ_{31} calculated as a function of the P_+ - P_- splitting energy for a fixed 50 meV S - P_- transition energy. τ_{31} and τ_{32} are calculated following Ref. 6 as a function of the corresponding transition energies, assuming a coupling strength of $g = 4.4$ meV. τ_{31} and τ_{32} correspond to a relaxation triggered by the disintegration of the one-phonon component of the polaron state and depends on its weight in the quasiparticle.^{4,6} τ_{32} is calculated following Ref. 7 using the electronic envelope wave functions reported in Fig. 1. This fast relaxation, through the emission of an acoustic phonon,

occurs provided that the P_+ - P_- energy separation be small enough. Whereas τ_{21} and τ_{31} weakly depend on P_+ - P_- splitting and remain in the 45–90 ps range, τ_{32} can be strongly reduced for small splitting, with τ_{32} as short as 6 ps at 3 meV. We show in Fig. 2(b) that this is a favorable configuration to obtain optical gain. Note that these times correspond to the times measured in InAs/GaAs quantum dots at the energy of the s - p transition around 20–25 μm .^{6,7,20}

The optical gain g_{12} reported in Fig. 2(b) is calculated by solving optical Bloch equations in the incoherent regime (population rate equations) and steady state conditions considering only the population terms n_1 , n_2 , and n_3 for the three involved levels in a single quantum dot and integrated over the inhomogeneous distribution: $dn_3/dt = \sigma_{13}(n_1 - n_3)I_{13}/h\nu_{13} - (1/\tau_{32} + 1/\tau_{31})n_3$ and $dn_2/dt = n_3/\tau_{32} - n_2/\tau_{21}$. It is assumed, through the relation $n_1 + n_2 + n_3 = n_0$, that each QD in the distribution is populated with only one electron ($n_0 = 1$). E_{ij} , E_{ij}^0 , σ_{ij} , τ_{ij} , $\hbar\Gamma_{ij}$, I_{ij} , and $h\nu_{ij}$ are the $i \rightarrow j$ ISLT energy, $i \rightarrow j$ ISLT distribution mean energy, cross section, relaxation time, homogeneous half width at half maximum (HWHM), and closely resonant optical field intensity and energy, respectively. At infinite pump intensity, the normalized population inversion does not depend on the transition energies and reads $(n_2 - n_1)/n_0 = (1 - \tau_{32}/\tau_{21})/(1 + 2\tau_{32}/\tau_{21})$ showing that $\tau_{32} < \tau_{21}$ is a necessary condition to achieve population inversion and optical gain.

The contribution of one quantum dot to the gain reads $g_{12}^{\text{One QD}} = h\nu_{12}/E_{12}\sigma_{12}^0(n_2 - n_1)\pi\hbar\Gamma_{12}L(h\nu_{12} - E_{12})$, where L is a normalized Lorentzian of HWHM $\hbar\Gamma_{12}$ and $\sigma_{ij}^0 = E_{ij}^0/(\hbar\Gamma_{ij})d_{ij}^2/(\hbar n c \epsilon_0)$ the absorption cross section of the $i \rightarrow j$ ISLT where d_{ij} , \hbar , n , c , and ϵ_0 are the dipole length, reduced Planck constant, material index ($n = 3.3$), vacuum light speed, and permittivity. In order to take into account the inhomogeneous nature of ISL absorption, the individual QD gain is integrated over a 3 meV HWHM Gaussian distribution of energies E_{ij} , peaked at E_{ij}^0 , and assuming a constant relative P_+ - P_- splitting ($E_{23}/E_{12} = E_{23}^0/E_{12}^0$ for all dots). The number of QD planes is 80, which is a realistic figure already used experimentally.⁷ The thick line in Fig. 2(b) corresponds to $\hbar\Gamma_{ij} = \hbar/(5 \text{ ps})$, $E_{12}^0 = 50$ meV, $E_{13}^0 = 53$ meV, $d_{12} = 3.4 e \text{ nm}$, $d_{13} = 3.3 e \text{ nm}$, $n_0 = 4 \times 10^{10} \text{ cm}^{-2}$. In order to give an expression of g_{12} in cm^{-1} unit, a monomode waveguide geometry is assumed with a mode width of $L = 6 \mu\text{m}$.²¹ Positive optical gains in the range 0–330 cm^{-1} are predicted for an E_{23} energy separation below 5.8 meV. In this regime the relaxation of the polaron from the P_+ to the P_- state is sufficiently fast as compared to the relaxation of the polaron from P_- to the ground state, to lead to a greater accumulation of the quasiparticle in the P_- state as compared to the ground state. Note that such a favorable configuration where τ_{21} is shorter than τ_{32} has been experimentally reported in Ref. 7.

Figure 3 reports in log scale the I_{13} pump intensity dependence of the g_{12} gain. The dependence of the gain with the optical intensity strongly depends on the inhomogeneous nature of the ISLTs. It goes from a $I \rightarrow 1/(1 + I/I^s)$ law for a homogeneous transition (I^s is the transition saturation intensity), to a softer $I \rightarrow 1/\sqrt{1 + I/I^s}$ dependence for an inhomogeneous transition.²² The inhomogeneous nature of intraband absorption in InAs/GaAs quantum dot ensembles is not *a priori* straightforward. Experimental information correlated to theoretical prediction about the T_2 dephasing time of intersublevel transitions have been given only very recently

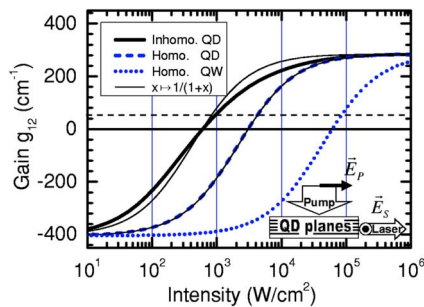


FIG. 3. Optical gain g_{12} as a function of the pump power density I_{13} at $E_{21}^0=50$ meV and for $E_{32}^0=3$ meV, in an inhomogeneous QD ensemble (thick full line), homogeneous QD ensemble (dashed line), and for homogeneous QW ISLTs of same total oscillator strength (dotted line). The $x \rightarrow \sqrt{1+x}$ dependence is depicted as a thin line. The horizontal dashed line corresponds to total waveguide losses $\alpha_{\text{GaAs}} - \ln(R)/L = 55 \text{ cm}^{-1}$. The inset describes the pumping and emission waveguide configuration.

with typical dephasing time of 5 ps for the s - p transition corresponding to homogeneous line width of only $\sim 250 \mu\text{eV}$, much smaller than the typical 6 meV spectral width of the absorption.⁸ This is illustrated in Fig. 3 in three different cases. The thick line depicts the gain dependence as calculated from a inhomogeneous distribution of QDs all exhibiting long $T1$ relaxation times of $\tau_{21}=46$ ps, $\tau_{31}=63$ ps, $\tau_{32}=5.6$ ps, and a $T2$ time of 5 ps ($E_{P+P-}=3$ meV in Fig. 2). The dashed line represents the dependence for a distribution of QDs with the same spectral width and oscillator strength than the inhomogeneous distribution but with a homogeneous broadening, assuming a $T2$ time of only 300 fs,²³ i.e., a homogeneous full width at half maximum of 4.24 meV, and a infinitely small inhomogeneous width. At last the dash-dotted line reports the gain dependence of the previous case after arbitrarily dividing the $T1$ relaxation times by a factor of 20 ($\tau_{21}=2.3$ ps, $\tau_{31}=3.2$ ps, $\tau_{32}=280$ fs), hence roughly mimicking the gain of a QW of a similar subband structure, with relatively short $T1$ and $T2$ times and equivalent dipole lengths of 3.4 nm.¹⁷ As compared to the QW case, the inhomogeneous QD case presents a 600 W/cm^2 transparency intensity two orders of magnitude smaller. This decrease of the transparency intensity results from two factors: the long $T1$ relaxation time of ISLTs and the relatively long dephasing time $T2$ of the transition. This transparency intensity reduction is expected from the longer relaxation and dephasing times in QDs than in QWs, following the ISLT saturation intensity expression $I_{12}^s = \hbar \Gamma_{12} n c \epsilon_0 / (2 \tau_{12} d_{12}^2)$.

At last, we consider the possibility of laser effect based on a perfect monomode waveguide structure at $25 \mu\text{m}$ and optical pumping at $23 \mu\text{m}$. In this case, the main considered source of losses are the bulk GaAs two phonon absorption²⁴ ($\alpha_{\text{GaAs}} < 15 \text{ cm}^{-1}$) reported at 20 K in Fig. 2(b) as a dashed line and the limited reflection coefficient at the end facets $R=28\%$. This situation differs from the QW case, where one of the main sources of loss is the free carrier absorption of the high density carriers trapped into the subband continua. Accounting for a propagation length of $L=0.5$ mm and a threshold gain condition $g_{12} - \alpha_{\text{GaAs}} + \ln(R)/L = 0$, lasing is predicted above 930 W/cm^2 pump intensity and below a $P_+ - P_-$ separation energy of 5.3 meV.

In conclusion, a Ruby-type three level scheme is proposed to realize an intersublevel polaron laser with InAs/GaAs self-assembled quantum dots. TE polarized op-

tical gain up to 330 cm^{-1} at 50 meV ($24.8 \mu\text{m}$) is predicted in an in-plane monomode waveguide geometry with 80 quantum dot planes and a threshold as low as 930 W/cm^2 is predicted in this configuration. The scheme relies on slow polaron relaxation above the phonon energy and fast polaron relaxation between closely space levels assisted by irreversible emission of acoustical phonons. The proposed optically pumped laser assumes the availability of a pump laser in resonance with the S - $P+$ transition around $23 \mu\text{m}$ wavelength. The scheme ideas can be extended at shorter wavelength, provided that the conditions $\tau_{32} < \tau_{21}$ for laser operation be fulfilled. Relaxation time engineering in QDs is suitably realized through LO-phonon disintegration and irreversible acoustic phonon emission. The scheme also directly opens the route of experimental investigation of intersublevel optical gain in quantum dots, in particular using a two-color free-electron laser.¹⁸

Parts of this work are funded by the SANDiE Network of Excellence of the European Commission, Contract No. NMP4-CT-2004-500101.

- ¹J. Faist, F. Capasso, D. S. Sivco, C. Sirtori, A. L. Hutchinson, and A. Y. Cho, *Science* **264**, 553 (1994).
- ²D. Hofstetter and J. Faist, *Top. Appl. Phys.* **89**, 61 (2003)
- ³R. Köhler, A. Tredicucci, F. Beltram, H. E. Beere, E. H. Linfield, A. G. Davies, D. A. Ritchie, R. C. Iotti, and F. Rossi, *Nature (London)* **417**, 156 (2002).
- ⁴X.-Q. Li, H. Nakayama, and Y. Arakawa, *Phys. Rev. B* **59**, 5069 (1999).
- ⁵S. Hameau, Y. Guldner, O. Verzellen, R. Ferreira, G. Bastard, J. Zeman, A. Lemaître, and J. M. Gérard, *Phys. Rev. Lett.* **83**, 4152 (1999).
- ⁶S. Sauvage, P. Boucaud, R. P. S. M. Lobo, F. Bras, G. Fishman, R. Prazeres, F. Glotin, J.-M. Ortéga, and J.-M. Gérard, *Phys. Rev. Lett.* **88**, 177402 (2002).
- ⁷E. A. Zibik, L. R. Wilson, R. P. Green, G. Bastard, R. Ferreira, P. J. Philips, D. A. Carder, J.-P. R. Wells, J. W. Cockburn, M. S. Skolnick, M. J. Steer, and M. Hopkinson, *Phys. Rev. B* **70**, 161305R (2004).
- ⁸F. Bras, S. Sauvage, G. Fishman, P. Boucaud, J.-M. Ortega, and J.-M. Gérard, *Europhys. Lett.* **70**, 390 (2005).
- ⁹N. S. Wingreen and C. A. Stafford, *IEEE J. Quantum Electron.* **33**, 1170 (1997).
- ¹⁰C.-F. Hsu, J.-S. O, P. Zory, and D. Botez, *IEEE J. Sel. Top. Quantum Electron.* **6**, 491 (2000).
- ¹¹I. A. Dmitriev and R. A. Suris, *Phys. Status Solidi A* **202**, 987 (2005).
- ¹²S. Sauvage and P. Boucaud, *C. R. Phys.* **4**, 1133 (2003).
- ¹³S. Hameau, J. N. Isaia, Y. Guldner, E. Deleporte, O. Verzellen, R. Ferreira, G. Bastard, J. Zeman, and J.-M. Gérard, *Phys. Rev. B* **65**, 085316 (2002).
- ¹⁴Ph. Lelong and S. H. Lin, *Appl. Phys. Lett.* **81**, 1002 (2002).
- ¹⁵M. A. Migliorato, D. Powell, S. L. Liew, A. G. Cullis, P. Navaretti, M. J. Steer, M. Hopkinson, M. Fearn, and J. H. Jefferson, *J. Appl. Phys.* **96**, 5169 (2004).
- ¹⁶T. Maiman, *Nature (London)* **187**, 493 (1960).
- ¹⁷J. Ulrich, J. Kreuter, W. Schrenk, G. Strasser, and K. Unterrainer, *Appl. Phys. Lett.* **80**, 3691 (2002).
- ¹⁸O. Gauthier-Lafaye, S. Sauvage, P. Boucaud, F. H. Julien, R. Prazeres, F. Glotin, J.-M. Ortega, V. Thierry-Mieg, R. Paniel, J. P. Leburton, and V. Berger, *Appl. Phys. Lett.* **70**, 3197 (1997).
- ¹⁹C. Kammerer, S. Sauvage, G. Fishman, P. Boucaud, G. Patriarche, and A. Lemaître, *Appl. Phys. Lett.* **87**, 173113 (2005).
- ²⁰F. Bras, P. Boucaud, S. Sauvage, G. Fishman, and J.-M. Gérard, *Appl. Phys. Lett.* **80**, 4620 (2002).
- ²¹The spatial mode width is defined as $1/L = nE^2 / \int nE^2$, where E is the electric field. It corresponds to the overlapping of the mode with one QD plane.
- ²²G. Beadie, W. S. Rabinovich, D. S. Katzer, and M. Goldenberg, *Phys. Rev. B* **55**, 9731 (1997).
- ²³J. Faist, C. Sirtori, F. Capasso, L. Pfeiffer, and K. W. West, *Appl. Phys. Lett.* **64**, 872 (1994).
- ²⁴W. Cochran, S. J. Fray, F. A. Johnson, J. E. Quarrington, and N. Williams, *J. Appl. Phys.* **32**, 2102 (1961).